



ELSEVIER

Physica E 1 (1997) 304–309

PHYSICA E

Resistance of molecular nanostructures

Weidong Tian^a, Supriyo Datta^{a,*}, Seunghun Hong^b, R.G. Reifenger^b,
J.I. Henderson^c, C.P. Kubiak^c

^a*School of Electrical and Computer Engineering, Purdue University, W. Lafayette, IN 47907-1285, USA*

^b*Department of Physics, Purdue University, W. Lafayette, IN 47907-1285, USA*

^c*Department of Chemistry, Purdue University, W. Lafayette, IN 47907-1285, USA*

Abstract

This paper describes a theoretical model that can be used to calculate the current–voltage (I – V) characteristics of molecular monolayers as measured between two contacts. Numerical results are presented for α , α' -xylyl dithiol showing that the I – V characteristics are sensitive to two parameters: the equilibrium Fermi energy, E_f , and the voltage division factor, η , which determines the shift in the molecular energy levels in response to the applied bias. Experimental data are presented showing good agreement with the theory. © 1997 Elsevier Science B.V. All rights reserved.

Keywords: Self-assembled monolayers (SAMs); Scanning tunneling microscopy (STM); Current–voltage spectroscopy

1. Introduction

Molecular wires based on alkane chains have large HOMO–LUMO gaps (5 eV and greater) and are relatively insulating [1]. On the other hand, molecular wires based on conjugated polymers like poly-paraphenylene have a small ([2–4] eV) HOMO–LUMO gap and behave much like ordinary semiconductors. In the solid state they have been doped to attain near-metallic levels of conductivity and used to make electroluminescent devices and transistors [2]. The conduction process in such bulk plastics is dominated by relatively complex processes such as inter-chain transfer and inter-particle hopping. By contrast,

recent experiments on self-assembled monolayers (SAMs) of these molecules [3] allow us to study the intrinsic conduction mechanisms in individual molecular chains which is of great interest to basic science [4–9]. In this paper we describe a theoretical model for the current–voltage (I – V) characteristics of such conjugated polymer chains as measured between two contacts and present some of our experimental results on α , α' -xylyl dithiol (see Fig. 1a).

We assume that the molecular chains are short enough such that polaronic effects are not significant. Also, we assume that the level broadening is larger than the single-electron charging energy U so that any charging effects can be accounted for with a self-consistent field approach. With these assumptions one can use the basic picture described in Refs. [10–14] and evaluate the I – V relation from the

* Corresponding author.

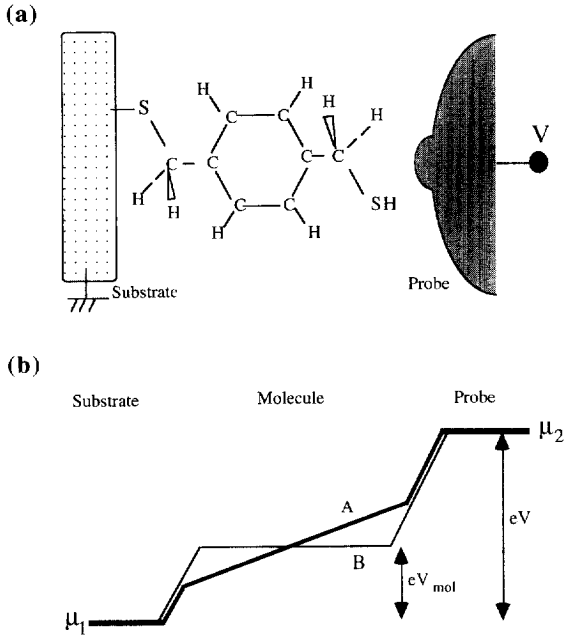


Fig. 1. (a) Self-assembled monolayer of *z, z'*-xylyl dithiol on a gold substrate (only one molecule of the monolayer is shown for clarity). Also shown schematically is a second contact used to probe the current-voltage characteristics. (b) Expected spatial profile of the electrostatic potential (A) and an idealized approximation (B) that provides insight into its effect on the *I–V* characteristics (after Ref. [15]).

expression

$$\begin{aligned}
 I &= \frac{2e}{h} \int_{-\infty}^{\infty} dE T(E) [f(E - \mu_1) - f(E - \mu_2)] \\
 &\cong \frac{2e}{h} \int_{\mu_2}^{\mu_1} dE T(E). \tag{1.1}
 \end{aligned}$$

Here, $T(E)$ is the transmission function from the substrate to the tip, $f(E)$ is the Fermi function. The primary purpose of this paper is to fill in two crucial details that are needed to compare the predictions from Eq. (1.1) with experiment.

Where is the Fermi energy? This is crucial in determining low-bias resistance which is related to the transmission at the equilibrium Fermi energy, E_f , through the Landauer formula [15]

$$\begin{aligned}
 R^{-1} &= [\partial I / \partial V]_{V \rightarrow 0} \\
 &= (2e^2/h) T(E_f). \tag{1.2}
 \end{aligned}$$

It is clear that the resistance will be relatively low if the Fermi energy were to lie close to the energy of one of the molecular orbitals. In Section 2 we will describe how the Fermi energy can be located from a knowledge of the number of electrons in the molecule.

Where is the voltage drop? We find that the electric field inside the molecule due to the applied bias has a qualitative effect on the *I–V* characteristics and has to be included even for a zero-order estimate. Typically for small bias there is hardly any change in the charge inside the molecule so that the change in the electrostatic potential $\delta\phi(\mathbf{r})$ can be obtained by solving the Laplace equation $\nabla \cdot (\epsilon \nabla \delta\phi) = \delta\rho \cong 0$. If we view the probe and the gold substrate as the two plates of a parallel-plate capacitor then the electrostatic potential will vary as shown in profile A of Fig. 1b. The electric field (slope of the potential) is lowered inside the molecule due to its higher dielectric constant (estimated to be ~ 3) relative to that in the gaps at the ends. The effect of this electric field is easily understood if we approximate the potential profile by profile B. The molecular energy levels then simply float up by an amount eV_{mol} equal to the average electrostatic potential in the molecule. We find that more accurate calculations using profile A agree well with the results obtained from this simple picture.

Based on this simple picture, we can take the molecular energy levels as a fixed reference and let the substrate float down by eV_{mol} so that the applied bias is split between the two junctions as shown in Fig. 2:

$$\mu_1 = E_f - \eta eV \tag{1.3a}$$

$$\mu_2 = E_f + (1 - \eta)eV \tag{1.3b}$$

(note that $e = -1.6 \times 10^{19}$ C) where the factor η describes how the electrostatic potential difference V is divided between the two junctions: $\eta \equiv V_{\text{mol}}/V$. In break junctions [8], the two contacts are nominally symmetric and the factor η should be close to 0.5. In STM measurements, this factor should be smaller since the probe is farther from the molecule than the substrate. But the decrease is linear (not exponential) with probe distance. Since the probe has to be within a few angstroms from the end of the molecule in order for the current to be measurable, the factor η can be as large as 0.5 even in STM measurements.

It is easy to see that the factor η can have a profound effect on the measured *I–V* characteristics

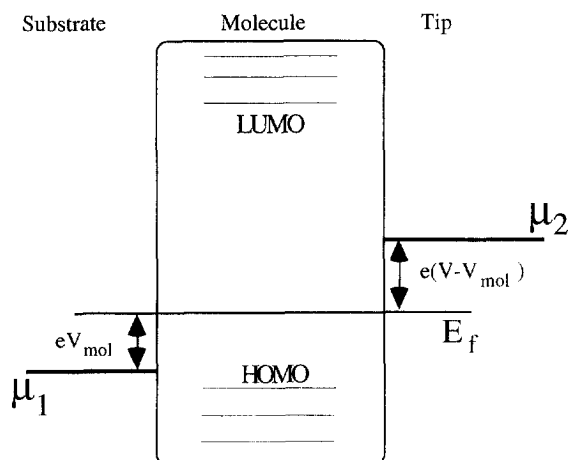


Fig. 2. Taking the molecular potential as the reference, μ_1 moves down by eV_{mol} while μ_2 moves up by $e(V - V_{\text{mol}})$, where V_{mol} is the average electrostatic potential in the molecule.

[16]. If η were zero, as is often assumed, then μ_1 would remain fixed with respect to the molecule. The molecule then conducts strongly as the electrochemical potential in the tip, μ_2 , approaches the LUMO (for negative sample voltage) or the HOMO (for positive sample voltage). This leads to a strongly asymmetric I - V characteristic since the HOMO is a sulfur-based level that couples strongly to the gold while the LUMO is a ring-based level that couples only weakly. But if we assume $\eta = 0.5$, we get a symmetric I - V since the molecule can conduct through the HOMO for both polarities (assuming E_f to be closer to the HOMO than the LUMO).

We will describe the theoretical model in Section 2. In Section 3 we present numerical results based on this model for the I - V characteristics of α , α' -xylyl dithiol as a function of two parameters: the equilibrium Fermi energy, E_f , and the voltage division factor, η . We also present experimental results for this molecule showing a good agreement with the theory.

2. Theoretical model

We use the extended Huckel method [16] to obtain the Hamiltonian (H) for the molecule along with six gold atoms at each end whose geometry (see Fig. 3) reflects the correct chemical bonding of the

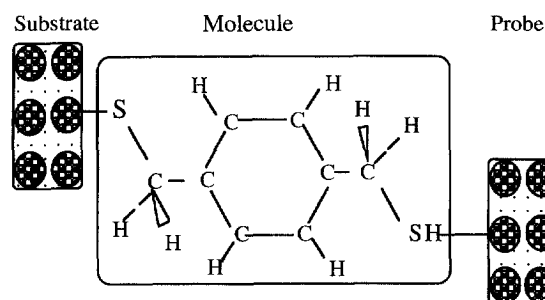


Fig. 3. Schematic diagram illustrating the extended "molecule".

thiol group to the (111) gold surface. Self-energy functions Σ_1 and Σ_2 are added to the gold atoms on the left and right, respectively, to "convert" each of these into infinite contacts [17]. In general, these are energy-dependent functions with off-diagonal elements. However, a reasonably good approximation can be obtained using a simple diagonal self-energy function whose diagonal elements are non-zero only for the gold atoms in question. For our calculations, we choose the non-zero diagonal elements to be $-5i$ to reflect the correct surface density of states of gold [18]. The eigenenergies of $(H + \Sigma_1 + \Sigma_2)$ are complex: $E_i = \varepsilon_i + i\gamma_i$. The real part (ε_i) is the energy of a molecular orbital while the imaginary part (γ_i) represents its broadening due to the coupling to the metal and describes how effectively the orbital couples to the metallic reservoirs.

We also add a self-energy function Σ_p to the molecule to reflect the broadening of energy levels due to the coupling to molecular vibrations. The simplest approximation would be to add a diagonal self-energy with its diagonal elements equal to half the average broadening of an energy level (~ 0.01 – 0.1 eV). A better approximation is to let the broadening at each energy be proportional to the density of states at that energy. This requires a self-consistent evaluation of the Greens function, G , from the relations

$$G = (E - H - \Sigma_1 - \Sigma_2 - \Sigma_p)^{-1} \quad (2.1)$$

and

$$\Sigma_p = D_0 G, \quad (2.2)$$

where D_0 is a constant that reflects the strength of the coupling of the electronic levels to the molecular

vibrations. In this paper $D_0 = 0.05$ is used, the precise value has no significant effect on the result.

Note that each of the quantities appearing in Eq. (2.1) is represented by a matrix of size $(N \times N)$, N being the number of atomic orbitals. For the molecule shown in Fig. 3, this number is 61: four orbitals each for the eight carbon atoms and two sulfur atoms (40) plus one orbital each for the nine hydrogen atoms and twelve gold atoms (21). Note that we use only one s-orbital for each of the gold atoms, since it is known that the DOS around the Fermi energy is dominated by the s-band. It should be mentioned that there are a few subtle issues arising from the non-orthogonality of the atomic orbitals that we are not discussing here.

From the Greens function we can calculate the spectral function (A) whose diagonal elements represent the density of states (DOS) associated with the different atomic orbitals. The total density of states is obtained from the trace of the spectral function:

$$A = i(G - G^+), \quad (2.3)$$

$$N(E) = \text{trace}(A)/\pi. \quad (2.4)$$

2.1. Equilibrium Fermi energy, E_f

Once we have the total DOS, it is a relatively simple matter to locate the Fermi energy so as to yield the correct number of electrons for the molecule (appropriately extended to include a few end atoms as shown in Fig. 3). For the molecule shown in Fig. 1a, the total number of electrons n_T is equal to 65: four electrons each for the eight carbon atoms (32), six electrons each for the two sulfur atoms (12) plus one electron each for the nine hydrogen atoms and twelve gold atoms (21). The Fermi energy is fixed by the requirement

$$n_T(E_f) = 65 = \int_{-\infty}^{E_f} dE N(E). \quad (2.5)$$

It should be noted that a fractional amount of charge (which could be transferred from an ambient species for example) could change the location of E_f significantly since $N(E)$ is relatively small inside the gap. The broadening of the levels also has a significant effect on the Fermi energy. It thus seems advisable to treat E_f as a “fitting parameter” (within reasonable limits) when trying to explain experimental $I-V$ curves.

2.2. Current-voltage ($I-V$) characteristics

The $I-V$ characteristics can be obtained from Eq. (1.1) if we know the transmission function $T(E)$ which can be calculated from a knowledge of H and Σ as described in Ref. [11]. However, there are two important refinements that need to be made. Firstly, in calculating the Greens function G from Eq. (2.1), it is important to include the electrostatic potential profile (see profile A, Fig. 2) in the Hamiltonian H . As a result the transmission function in Eq. (1.1) is not simply a function of energy but a function of bias as well. If we use the approximate profile B (instead of A) then it is easy to see the effect of the bias: it simply shifts the transmission function in energy by eV_{mol} ; i.e.,

$$T(E, V) \cong T(E + eV_{\text{mol}}, V = 0). \quad (2.6)$$

For bias values less than 4 V, we find that this is a reasonably good approximation.

Secondly, we have included scattering through the self-energy function Σ_p . If we now simply calculate the transmission from contact 1 to contact 2, we will get the coherent current. But in addition there is an incoherent current composed of electrons that come in from contact 1, get scattered inside the molecule and finally reach contact 2. As first shown by Buttiker one can calculate the total transmission T from the relation

$$T = T_{21} + \frac{T_{2p}T_{p1}}{T_{p2} + T_{p1}}, \quad (2.7)$$

where the first term gives the coherent component, while the second term gives the incoherent component. The quantities appearing in Eq. (2.7) can be evaluated from a knowledge of the Greens function G [19]:

$$T_{mn} = \text{trace}(\Gamma_m G \Gamma_n G^-), \quad (2.8)$$

$$\text{where } \Gamma_{1,2,p} = i(\Sigma_{1,2,p} - \Sigma_{1,2,p}^+). \quad (2.9)$$

It should be mentioned that the approach we are using here to include scattering processes is only approximate. A proper treatment of inelastic scattering is relatively more complicated [20] and is not justified at this stage when we are trying to understand the broad features of the experimental data with a minimum number of “fitting” parameters.

3. Results and discussion

Fig. 4a–4c shows plots of $|I|$ versus V for the molecule in Fig. 1a calculated for three different values of the Fermi energy, E_f . For each value of E_f , we show calculations for three values of the voltage division factor η . The crosses in Fig. 4c show a typical experimental I – V curve which seems to be described well by the theoretical plot with $\eta = 0.5$ and $E_f - E_{\text{HOMO}} = 1.8$ eV. We also find good agreement between the shape of the theoretical I – V characteristics of phenyl dithiol calculated with $\eta = 0.5$ and the

experimental I – V data of Reed et al. obtained using break junctions [8]. But the experimentally observed current levels are smaller by about a factor of 100, possibly because the gold–sulfur bonds in a break junction are much weaker than what we expect for large area SAM's.

We have measured a few hundred I – V curves at different locations within the SAM with different tips. A vast majority of these curves are reasonable symmetric: the currents for equal values of positive and negative bias are within an order of magnitude (or less) of each other. Slight asymmetries can be

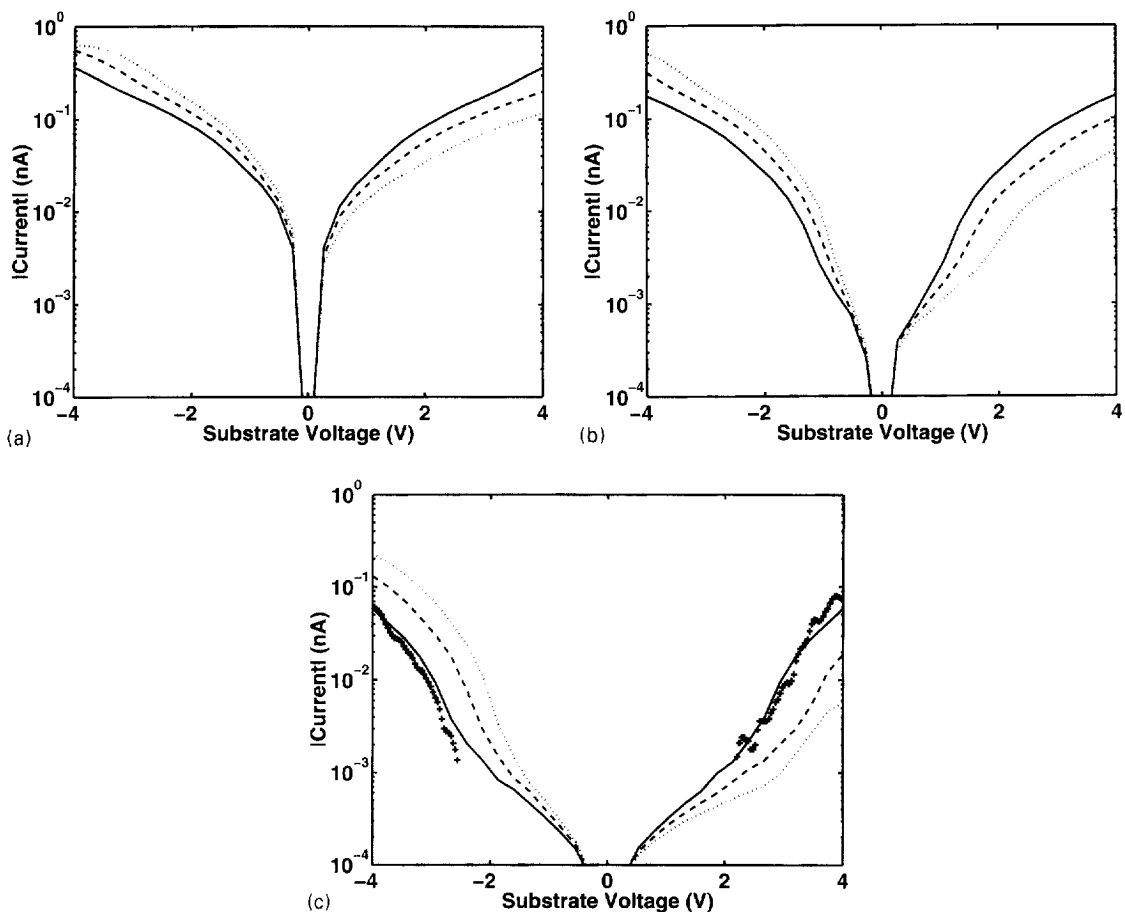


Fig. 4. Theoretical I – V characteristics for the molecule shown in Fig. 1 with $\eta = 0.5$ (solid), 0.4 (dashed) and 0.3 (dotted): (a) $E_f - E_{\text{HOMO}} = 0.5$ eV, (b) $E_f - E_{\text{HOMO}} = 1$ eV and (c) $E_f - E_{\text{HOMO}} = 1.8$ eV. The crosses in (c) show a typical experimental curve.

explained in terms of a small decrease in the value of η from the perfectly symmetric case ($\eta = 0.5$). Another consistent trend that we find is that as the tip is moved away from the molecule, the current for positive bias decreases *much faster* than that for negative bias. This is consistent with our theoretical predictions, since we expect η to decrease as the tip is withdrawn. It is evident from the theoretical plots in Fig. 4a–4c that for each value of E_f , the I – V curves are symmetric for $\eta = 0.5$. But with smaller values of η , the current for positive bias is reduced far more than that for negative bias, as observed experimentally with increasing tip–molecule distance. We have obtained similar results for a series of molecules with thiol and isocyanide endgroups with different numbers of phenyl rings, which will be published elsewhere.

Acknowledgements

It is a pleasure to thank R.P. Andres and D. Janes for their helpful comments throughout this study. This work was supported by the Army Research Office under a University Research Initiative Grant No. DAAL-03-92-G-0144.

References

- [1] U. Durig, O. Zuger, B. Michel, L. Haussling, H. Ringsdorf, *Phys. Rev. B* 48 (1993) 1711.
- [2] See, for example, articles in the MRS Bulletin, vol. 22, Materials Research Society, June 1997.
- [3] Y. Xia, G.M. Whitesides, *Adv. Mater.* 7 (1995) 471.
- [4] D.L. Klein, P.L. McEuen, J.E. Bowen Katari, R. Roth, A. Paul Alivisatos, *Appl. Phys. Lett.* 68 (1995) 2574.
- [5] C. Boudas, J.V. Davidovits, F. Rondelez, D. Vuillaume, *Phys. Rev. Lett.* 76 (1996) 4797.
- [6] L.A. Bumm, J.J. Arnold, M.T. Cygan, T.D. Dunbar, T.P. Burgin, L. Jones II, D.L. Allara, J.M. Tour, P.S. Weiss, *Science* 271 (1996) 1705.
- [7] R.P. Andres, T. Bein, M. Dorogi, S. Feng, J.I. Henderson, C.P. Kubiak, W. Mahoney, R.G. Osifchin, R.G. Reifengerger, *Science* 272 (1996) 1323.
- [8] M.A. Reed, C. Zhou, C.J. Muller, T.P. Burgin, J.M. Tour, *Science* 278 (1997) 252.
- [9] A. Dhirani, P.-H. Lin, P. Guyot-Sionnest, R.W. Zehner, L.R. Sita, *J. Chem. Phys.* 106 (1997) 5249.
- [10] C. Joachim, J.F. Vinuesa, *Europhys. Lett.* 33 (1996) 635, and references therein.
- [11] M.P. Samanta, W. Tian, S. Datta, J.I. Henderson, C.P. Kubiak, *Phys. Rev. B* 53 (1996) R7626.
- [12] M. Kemp, A. Roitberg, V. Mujica, T. Wanta, M.A. Ratner, *J. Phys. Chem.* 100 (1996) 8349.
- [13] V. Mujica, M. Kemp, A. Roitberg, M.A. Ratner, *J. Chem. Phys.* 104 (1996) 7296.
- [14] C.P. Tsu, R.A. Marcus, *J. Chem. Phys.* 106 (1997) 584.
- [15] S. Datta, W. Tian, S. Hong, R.G. Reifengerger, J.I. Henderson, C.P. Kubiak, *Phys. Rev. Lett.* 79 (1997) 2530.
- [16] R. Hoffman, *J. Chem. Phys.* 39 (1963) 1937.
- [17] S. Datta, *Electronic Transport in Mesoscopic Systems*, Ch. 2, Cambridge University Press, Cambridge, 1995 and references therein.
- [18] D.A. Papaconstantopoulos, *Handbook of the Band Structure of Elemental Solids*, Plenum Press, New York, 1996.
- [19] See Ref. [17], Ch. 3.
- [20] See Ref. [17], Ch. 8 and references therein.